

Down- and Up-Conversion Luminescent Nanorods**

By Leyu Wang, Peng Li, and Yadong Li*

The rapidly increasing health care is now challenging the development of fluorescent biolabel materials used in diagnostics and bioanalysis such as immunoassay, fluorescence imaging and DNA or toxin detection.^[1–5] Due to their multicolor emission, high brightness and long lifetime, lanthanide ions based luminescent nanomaterials have tremendous promise as indicators and photon sources for numerous applications such as biolabels, light-emitting devices, sensor technology, and low-threshold lasers.^[5–11] However, when they are used in polymer-based luminescence devices, their strong luminescence is often quenched by the organic compounds. Therefore, doping the luminescent rare-earth ions into inorganic host materials can efficiently maintain their novel luminescence.^[6] But if their surface is not coated with organic compounds, these lanthanide-doped inorganic materials can not be dispersed in organic environment, which will further limits their application in polymer-based devices. So, it is very important to successfully prepare the rare-earth doped inorganic nanocrystals with good dispersibility in organic solvents.

Up to now, lots of facile strategies have been developed for the preparation and application of the one-dimensional nanomaterials such as carbon nanotubes,^[12,13] semiconductor^[14–18] and metal^[19] nanocrystals, however, it is still a challenge for the synthesis of highly luminescent LaF₃ and NaLaF₄ nanorods with uniform shapes and sizes, high crystallinity, and especially controllable surface properties. Herein, we developed a facile one-pot strategy for the preparation of rare-earth doped lanthanum fluoride (LaF₃) and sodium lanthanum fluoride (NaLaF₄) nanorods with controllable sizes and shapes. By doping different rare-earth ions, these nanorods can emit strong downconversion and upconversion fluorescence. For the coating surfactants on the surfaces, these as-prepared nanocrystals are redispersible in nonpolar organic solvents such as cyclohexane to form a transparent colloidal solution, and can be easily aggregated by adding polar solvents such as ethanol, which facilitates their applications in polymer-based devices.^[6] Meanwhile, for their novel luminescence, they will also find great application in clinical and biological fields

In brief, in water-ethanol-oleic acid mixing system, with a facile solvothermal technology,^[20] we successfully prepared the LaF₃ and NaLaF₄ nanorods by tuning sodium fluoride content and reaction time. By doping Ce³⁺-Tb³⁺ and Yb³⁺-Er³⁺ ion-pairs, novel down- and up-conversion luminescence have been obtained, respectively. The crystal structure, shape and size of the resulting nanocrystals were quite sensitive to the reaction time, dopant concentration and NaF content. The results have been demonstrated by transmission electron microscopy (TEM) in Figure 1. In the case of low NaF content (2.0 mL, 1.0 mol L⁻¹) and 6 h, only the short nanorods were obtained (Fig. 1a and b). High NaF content (2.7 mL, 1.0 mol L⁻¹) and long reaction time (10 h) are beneficial for the formation of long nanorods (Fig. 1c and d). But with the elongation of the nanorods, their crystal phase has been already changed from LaF₃ (Fig. 1a and b) to NaLaF₄

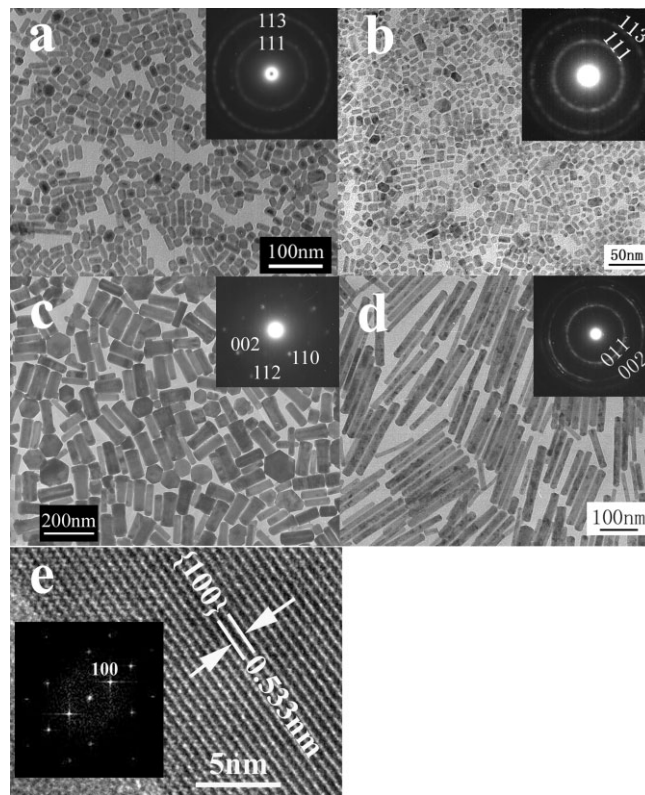


Figure 1. TEM images of LaF₃ (a and b) short nanorods and NaLaF₄ (c and d) long nanorods. b) and c) 18% Yb³⁺-2% Er³⁺ doped nanorods; a) and d) 5% Ce³⁺-5% Tb³⁺ doped nanorods; e) HRTEM of single nanorod selected from d; insets of a–d are the ED patterns; inset of e is the Fourier transform electron diffraction pattern from the HRTEM image.

[*] Prof. Y. Li, L. Wang, P. Li
Department of Chemistry, Tsinghua University
Beijing, 100084 (P.R. China)
E-mail: ydli@tsinghua.edu.cn

[**] This work was supported by NSFC (90606006), the Foundation for the Author of National Excellent Doctoral Dissertation of China and the State Key Project of Fundamental Research for Nanoscience and Nanotechnology (2006CBON0300).

(Fig. 1c and d). Moreover, the dopant concentration also influenced the aspect ratios of the nanorods, which has been demonstrated in Figure 1c (NaLaF₄:18%Yb³⁺-2%Er³⁺) and Figure 1d (NaLaF₄:5%Ce³⁺-5%Tb³⁺). The low resolution TEM images illustrate that the nanocrystals are highly crystalline and well dispersed. Their high crystallinity is also inferred from the high-resolution TEM (HRTEM) images (Fig. 1e) showing lattice fringes for the long NaLaF₄:Ce³⁺-Tb³⁺ nanorod, which indicates that the nanorods are single-crystal. The electron diffraction (ED) patterns are consistent with the hexagonal phase structure of LaF₃ and NaLaF₄ with strong ring patterns due to (111), (113) planes for LaF₃ (insets of Fig. 1a and b), and 011, 002 planes for NaLaF₄ (inset of Fig. 1d), respectively. Electron diffraction pattern of single NaLaF₄:Yb³⁺-Er³⁺ nanorod further indicates its high crystallinity (inset of Fig. 1c). It should be mentioned, in this work, if the water content is above 4 mL, the size and shape of the nanocrystals can not be reasonably controlled and few nanorods will be obtained.

The powder X-ray diffraction (XRD) analyses are in good agreement with the TEM results. Figure 2 shows the typical 2-theta X-ray diffraction (XRD) patterns of the as-prepared nanocrystals, which confirms the hexagonal structure of the

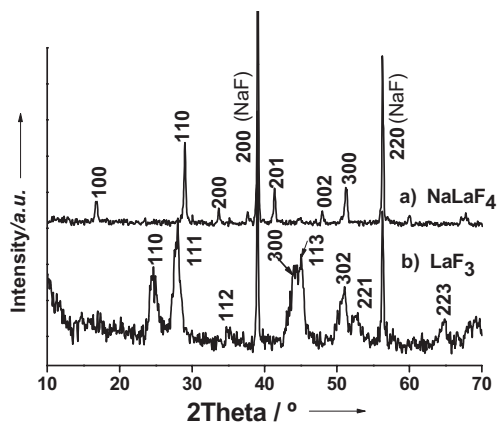


Figure 2. XRD patterns of the NaLaF₄ (a) and LaF₃ (b) nanorods.

LaF₃ and NaLaF₄ nanorods. From the XRD patterns, we can see that all of the reflections of short nanorods can be identified to the hexagonal LaF₃ structure with lattice parameters of $a = 7.163 \text{ \AA}$ and $c = 7.329 \text{ \AA}$ (JCPDS 72-1435). Meanwhile, all the peak positions and relative intensities of the long nanorods match well with those of hexagonal phase structure known from the bulk NaLaF₄ crystal (JCPDS card 75-1923) with crystal cell parameters of $a = 0.6179 \text{ nm}$ and $c = 0.3827 \text{ nm}$. Moreover, the excessive sodium fluoride also emerged in the XRD pattern. However, it should be mentioned that excessive sodium fluoride can be removed by water washing or filtration.

The as-prepared nanorods can be transparently dispersed in cyclohexane. This high degree of dispersibility may indicate

that the surface of the nanocrystals is covered with surfactants, which limits the growth of particles and stabilizes the agglomeration. For the coated surfactants, i.e., oleic acids, the as-prepared nanorods can be transparently redispersed in cyclohexane. The FTIR analysis has confirmed the existence of the coated oleic acid. As shown in Figure 3, the broadened signal of 3481 cm^{-1} can be attributed to $\nu_{\text{as}}(\text{O-H})$, the bands of 2923 and 2854 cm^{-1} are assigned to $\nu_{\text{as}}(\text{CH}_2)$ and $\nu_{\text{s}}(\text{CH}_2)$ of the long alkyl chain, respectively. Moreover, the 1678 cm^{-1}

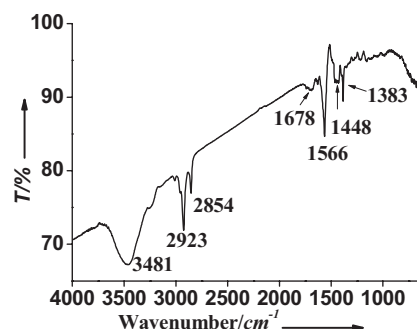


Figure 3. FTIR spectrum of the as-prepared nanorods.

is attributed to C=O stretching vibration frequency from the carboxyl of oleic acid. The bands at 1566 and 1448 cm^{-1} can also be assigned to the asymmetric (ν_{as}) and symmetric (ν_{s}) stretching vibration of the carboxylic group ($-\text{COOH}$) in the long strands of coated oleic acid, respectively. Moreover, the vibration signal of 1383 cm^{-1} is attributed to the $\delta(\text{CH}_3)$.

Figure 4 shows the emission and excitation spectra of the Ce³⁺-Tb³⁺ ion-pair codoped LaF₃ nanorods with a doping concentration of 5% Ce³⁺ and 5% Tb³⁺. The emission spectrum in the visible region was obtained by exciting the sample at 258 nm (Fig. 4b). The typical emission peaks of terbium were observed around 486 , 543 , 587 , and 619 nm assigned to the transitions of $^5\text{D}_4\text{-}^7\text{F}_J$ ($J = 6, 5, 4, 3$), respectively.^[9] Besides

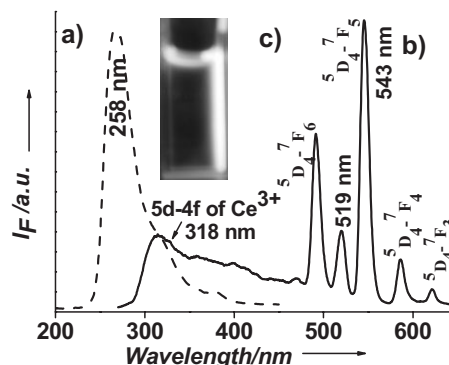


Figure 4. Excitation (a) and emission (b) spectra of the LaF₃:Ce³⁺-Tb³⁺ colloids. c) is the luminescence photograph obtained under UV lamp excitation. Here, the peak of 519 nm in emission line is the second order Rayleigh scattering of 258 nm excitation.

the typical emission of Tb^{3+} ions, the weak and broad emission around 318 nm can be attributed to the 5d–4f transition of Ce^{3+} ions.^[21] The dominant green emission corresponding to $^5\text{D}_4$ – $^7\text{F}_5$ transition is centered at 543 nm. It should be mentioned that the peak of 519 nm in emission line is the second order Rayleigh scattering of 258 nm excitation. Furthermore, the novel yellowish-green luminescence photo of the $\text{LaF}_3:\text{Ce}^{3+}\text{-Tb}^{3+}$ colloid is presented in Figure 4c. This naked-eye-visible luminescence again confirms the unique optical property of the as-synthesized $\text{LaF}_3:\text{Ce}^{3+}\text{-Tb}^{3+}$ nanorods. The strong excitation peak of $\text{LaF}_3:\text{Ce}^{3+}\text{-Tb}^{3+}$ colloids was centered around 258 nm (measured by collecting the emission at 543 nm), attributed to the 4f–5d transition of Ce^{3+} (Fig. 4a). It is well known that Ce^{3+} ions have a relatively broad absorption band from 200 to 300 nm with an allowed 4f–5d transition, and transfer their energy to the doped Tb^{3+} ions which emits the green fluorescence.^[5,10,22] The novel green emission indicates that an energy transfer from Ce^{3+} to Tb^{3+} occurs in the $\text{LaF}_3:\text{Ce}^{3+}\text{-Tb}^{3+}$ nanorods, as observed in the $\text{CeF}_3:\text{Tb}^{3+}$ ^[21] and $\text{LaPO}_4:\text{Ce}^{3+}\text{-Tb}^{3+}$ ^[22] nanoparticles. The unbelievably weak emission (not shown here) of $\text{LaF}_3:\text{Tb}^{3+}$ nanorods without cerium-doping further confirmed the importance of the energy transfer from Ce^{3+} to Tb^{3+} in $\text{LaF}_3:\text{Ce}^{3+}\text{-Tb}^{3+}$ nanocrystals. It is worthy noting that the $\text{Ce}^{3+}\text{-Tb}^{3+}$ ion-pair codoped NaLaF_4 long nanorods also demonstrates the same optical properties as that of $\text{LaF}_3:\text{Ce}^{3+}\text{-Tb}^{3+}$ nanorods and is not shown here for the sake of conciseness.

As we known, the abundant emission colors of lanthanide-based materials are attributed to the transitions within the 4f shell of the lanthanide ions. Meanwhile, these transitions are parity forbidden, which results in their novel optical properties such as long fluorescence lifetimes and low absorption cross-sections.^[6] However, their further applications in some organic surroundings are often hampered owing to the efficient quenching of this long-lived excited state in the presence of the high-energy vibrations of organic solvents, polymers or ligands. Therefore, to use these lanthanide-based materials in organic surroundings and maintain their novel luminescence, numerous attentions should be paid to the preparation of the lanthanide-doped inorganic materials with high crystallinity in that this strategy can efficiently shield these ions from the organic environments. Moreover, these luminescent inorganic materials should be coated with organic compounds to make them redispersible in organic solvents. Therefore, the lanthanide-based luminescent inorganic nanorods prepared in this work, will find great potential applications in the polymer-based devices such as displays and luminescent membrane, due to their novel luminescence and good redispersibility and processability in organic solvents.

To test the upconversion luminescence capabilities of the as-prepared LaF_3 and NaLaF_4 nanorods, the syntheses of $\text{Yb}^{3+}\text{-Er}^{3+}$ ion-pair codoped LaF_3 and NaLaF_4 nanorods were carried out. The emission spectrum of the LaF_3 nanorods shows the typical upconversion emission peaks of Er^{3+} excited with a 0–800 mW adjustable red laser excitation at 980 nm. As shown in Figure 5, the two emission bands of LaF_3

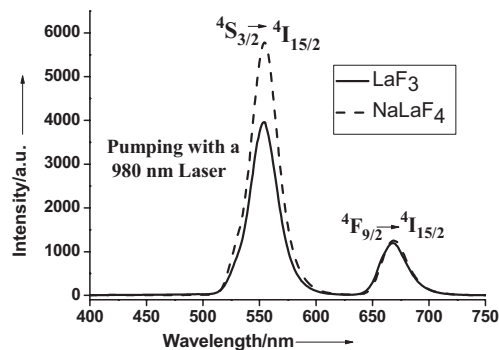


Figure 5. Upconversion emission spectra of the $\text{Yb}^{3+}\text{-Er}^{3+}$ ion-pair codoped LaF_3 and NaLaF_4 nanorods.

$\text{F}_3:\text{Yb}^{3+}(18\%)\text{-Er}^{3+}(2\%)$ nanorod powder are attributed to the transitions $^4\text{S}_{3/2}\text{-}^4\text{I}_{15/2}$ (~554 nm) and $^4\text{F}_{9/2}\text{-}^4\text{I}_{15/2}$ (~669 nm).^[3,23] The dominant green emission peak is centered at 554 nm assigned to the $^4\text{S}_{3/2}\text{-}^4\text{I}_{15/2}$ transition. Meanwhile, $\text{Yb}^{3+}(18\%)\text{-Er}^{3+}(2\%)$ ion-pair codoped NaLaF_4 nanorod powder demonstrates stronger yellowish-green upconversion emission than that of LaF_3 nanorods.

In summary, using a facile one-pot strategy, we prepared highly luminescent LaF_3 and NaLaF_4 nanorods. For the overlay of oleic acids on their surface, these nanocrystals can be easily dispersed in cyclohexane. Due to their high upconversion and downconversion luminescence, easy processing and simple fabricating, these luminescent inorganic nanocrystals, will find great potential applications in the polymer-based devices. They will also find potential bioapplications as luminescent biolabels in biological and medical fields.

Experimental

Synthesis of Nanorods: $\text{LaF}_3:\text{Ce}^{3+}\text{-Tb}^{3+}$ nanorods were synthesized with a facile solvothermal technology. In typical, 0.6 g of NaOH was dissolved into 2 mL of water, then 20 mL of ethanol and 10 mL of oleic acid was added under stirring, thereafter 0.9 mL of $\text{La}(\text{NO}_3)_3$ (0.5 mol L^{-1}), 50 μL of $\text{Ce}(\text{NO}_3)_3$ (0.5 mol L^{-1}), 50 μL of $\text{Tb}(\text{NO}_3)_3$ (0.5 mol L^{-1}), and 2.0 mL of sodium fluoride solution (NaF , 1 mol L^{-1}) were added and thoroughly stirred. Then the colloidal solution was transferred into a 50 mL Teflon-lined autoclave and heated at 190°C for 6 h. For the $\text{LaF}_3:\text{Yb}^{3+}\text{-Er}^{3+}$ nanorods, only the lanthanide ion content has been changed as 0.8 mL of $\text{La}(\text{NO}_3)_3$ (0.5 mol L^{-1}), 180 μL of $\text{Yb}(\text{NO}_3)_3$ (0.5 mol L^{-1}), 20 μL of $\text{Er}(\text{NO}_3)_3$ (0.5 mol L^{-1}), and other conditions are identical to that demonstrated above. By increasing the NaF content to 2.7 mL and prolonging the reaction time to 10 h, this novel procedure also has been applied for the preparation of NaLaF_4 nanorods. The final product was collected by centrifuging and washing with ethanol and cyclohexane.

Characterization: The size and morphology of the nanorods was observed by a JEOL JEM-1200EX transmission electron microscope (TEM) and a JEOL JEM-2010F high resolution transmission electron microscope (HRTEM). A Bruker D8-advance X-ray powder diffractometer with $\text{Cu K}\alpha$ radiation ($\lambda = 1.5418 \text{ \AA}$) was used for the characterization of phase purity and crystallinity of the samples. FTIR spectrum was conducted with a Nicolet 560 Fourier transform infrared spectrophotometer. Luminescence spectra were recorded on a Hitachi F-4500 fluorescence spectrophotometer with a xenon lamp source.

Upconversion fluorescence spectra were obtained on Hitachi F-4500 fluorescence spectrophotometer under the excitation of a 980 nm laser.

Received: January 18, 2007

Revised: March 28, 2007

Published online: September 20, 2007

-
- [1] W. C. W. Chan, S. M. Nie, *Science* **1998**, *281*, 2016.
- [2] L. Wang, C. Y. Yang, W. H. Tan, *Nano Lett.* **2005**, *5*, 37.
- [3] L. Y. Wang, R. X. Yan, Z. Y. Huo, L. Wang, J. H. Zeng, J. Bao, X. Wang, Q. Peng, Y. D. Li, *Angew. Chem. Int. Ed.* **2005**, *44*, 6054.
- [4] M. Bruchez, M. Moronne, P. Gin, S. Weiss, A. P. Alivisatos, *Science* **1998**, *281*, 2013.
- [5] F. Meiser, C. Cortez, F. Caruso, *Angew. Chem. Int. Ed.* **2004**, *43*, 5954.
- [6] J. W. Stouwdam, F. van Veggel, *Nano Lett.* **2002**, *2*, 733.
- [7] R. Sivakumar, F. van Veggel, M. Raudsepp, *J. Am. Chem. Soc.* **2005**, *127*, 12464.
- [8] S. Heer, O. Lehmann, M. Haase, H. U. Gudel, *Angew. Chem. Int. Ed.* **2003**, *42*, 3179.
- [9] L. Y. Wang, Y. D. Li, *Nano Lett.* **2006**, *6*, 1645.
- [10] P. R. Diamente, R. D. Burke, F. van Veggel, *Langmuir* **2006**, *22*, 1782.
- [11] H. X. Mai, Y. W. Zhang, R. Si, Z. G. Yan, L. D. Sun, L. P. You, C. H. Yan, *J. Am. Chem. Soc.* **2006**, *128*, 6426.
- [12] N. W. S. Kam, Z. A. Liu, H. J. Dai, *Angew. Chem. Int. Ed.* **2006**, *45*, 577.
- [13] Y. R. Lu, S. Bangsaruntip, X. R. Wang, L. Zhang, Y. Nishi, H. J. Dai, *J. Am. Chem. Soc.* **2006**, *128*, 3518.
- [14] P. J. Pauzauskie, A. Radenovic, E. Trepagnier, H. Shroff, P. D. Yang, J. Liphardt, *Nat. Mater.* **2006**, *5*, 97.
- [15] B. D. Yuhas, D. O. Zitoun, P. J. Pauzauskie, R. R. He, P. D. Yang, *Angew. Chem. Int. Ed.* **2006**, *45*, 420.
- [16] W. U. Huynh, J. J. Dittmer, A. P. Alivisatos, *Science* **2002**, *295*, 2425.
- [17] Y. Cui, Q. Q. Wei, H. K. Park, C. M. Lieber, *Science* **2001**, *293*, 1289.
- [18] J. Xiang, W. Lu, Y. J. Hu, Y. Wu, H. Yan, C. M. Lieber, *Nature* **2006**, *441*, 489.
- [19] K. B. Lee, S. Park, C. A. Mirkin, *Angew. Chem. Int. Ed.* **2004**, *43*, 3048.
- [20] X. Wang, J. Zhuang, Q. Peng, Y. D. Li, *Nature* **2005**, *437*, 121.
- [21] Z. L. Wang, Z. W. Quan, P. Y. Jia, C. K. Lin, Y. Luo, Y. Chen, J. Fang, W. Zhou, C. J. O'Connor, J. Lin, *Chem. Mater.* **2006**, *18*, 2030.
- [22] K. Riwotzki, H. Meysamy, H. Schnablegger, A. Kornowski, M. Haase, *Angew. Chem. Int. Ed.* **2001**, *40*, 573.
- [23] L. Y. Wang, Y. D. Li, *Chem. Commun.* **2006**, 2557.
-